Nonlinear Electrokinetic Methods of Particles and Cells

Blanca H. Lapizco-Encinas^{1,*}

¹Microscale Bioseparations Laboratory and Biomedical Engineering Department, Rochester Institute of

Technology, Rochester NY, USA

*Correspondence should be addressed to the following author:

Blanca H. Lapizco-Encinas (PhD)

Professor, Microscale Bioseparations Laboratory and Biomedical Engineering Department

Rochester Institute of Technology, Institute Hall (Bldg. 73), Room 3103

160 Lomb Memorial Drive, Rochester, NY 14623-5604

Phone: 585-475-2773 (Work)

Email: bhlbme@rit.edu

*** All figure permissions are included in this submission ***

Abstract

Nonlinear electrokinetic phenomena offer label-free, portable, and robust approaches for particle and cell assessment, including selective enrichment, separation, sorting and characterization. The field of electrokinetics has evolved substantially since the first separation reports by Arne Tiselius in the 1930s. The last century witnessed major advances in the understanding of the weak-field theory, which supported developments in the use of linear electrophoresis and its adoption as a routine analytical technique. More recently, advances in the understanding of the strong-field theory enabled the development of nonlinear electrokinetic techniques such as electrorotation, dielectrophoresis and nonlinear electrophoresis. The present review discusses the operating principles and recent applications of these three nonlinear electrokinetic phenomena for the analysis and manipulation of particles and cells and provides the reader with an overview of some of the latest developments in the field of nonlinear electrokinetics.

Keywords:

Dielectrophoresis

Electroosmosis

Electrophoresis

Electrokinetics

Electrorotation

Microfluidics

1

1. INTRODUCTION

Electrokinetics offers a wide array of methodologies for manipulating and assessing particles, including bioparticles, such as macromolecules and microorganisms. Electrophoresis is the most known electrokinetic mechanism, simply described as the migration of a charged particle toward the electrode with the opposite polarity, relative to a stationary fluid, under the influence of an electric field. Electrophoresis is almost 100 years old as it was first developed by Arne Tiselius in the 1930s for separating colloids and proteins (1).

The applications of electrophoresis and all electrokinetic techniques have grown substantially since the 1930s, as a plethora of distinct electrophoresis modes have been developed, and other electrokinetic techniques such as electrorotation and dielectrophoresis have been introduced into the field. These two later phenomena are related, as both result from the formation of a dipole in the particle. Electrorotation describes the rotation of target particles under the effect of rotating electric fields, while dielectrophoresis results in the migration of particles caused by polarization effects in nonuniform electric fields (1–3).

The advances in microfabrication and microelectrode technology enabled the development of new electrokinetic-based microfluidic methodologies for the analysis and assessment of particles and microorganisms (4). These new approaches ranged from enriching, sorting, trapping, to isolating a wide array target particles, ranging from macromolecules to nematodes (5–19). Electrokinetic-based methodologies are suitable for a variety of applications, from biomedical and clinical assessments (20, 21) to water quality (22, 23) and food safety analysis (24). Thus, electrokinetic-based methods have opened new possibilities in the field of bioanalysis, as they can work across several size scales of target particles and can be used in a wide range of distinct applications. Furthermore, these methods do not require the use of labels or tags, as electrokinetic phenomena exploit the physical properties of the target particles for detection and separation. Very few techniques offer this high degree of flexibility in terms of target particles, simplicity, and range of applications.

Electrokinetic methodologies are commonly classified as linear and nonlinear, as described by their dependance on the electric field magnitude. Linear electrokinetic phenomena (also called first kind) are those that depend on permanent surface charge and whose magnitude grow linearly with the electric field magnitude (25). Examples of linear electrokinetic phenomena are linear electrophoresis and electroosmotic flow, the former is exerted on electrically charged particle and the latter describes the motion of liquid, both phenomena occur under the influence of an electric field (26).

Nonlinear electrokinetic phenomena (also called of the second kind) are those that depend on the bulk charge and have a nonlinear dependence with the electric field magnitude (25). The present review article discusses the use of nonlinear electrokinetic techniques for the assessment of particles and cells. This review article discusses the nonlinear electrokinetic phenomena of electrorotation, dielectrophoresis and nonlinear

electrophoresis, covering both DC-electrokinetics and AC-electrokinetics, and the combination of AC and DC electric fields. The recent findings on insulator-based electrokinetic systems that combine linear and nonlinear effects by employing electrically insulating are also examined in detail.

Discussed here is the evolution of the field of electrokinetics, which is transitioning from mainly employing linear electrokinetic phenomena, to a significant use of nonlinear electrokinetic effects. As recently highlighted by Khair (27), the 20th century was marked by a significant growth in the field of linear electrokinetics, during the 20th century the fundamental understanding of the weak-field theory was developed. Electrophoretic techniques such as gel-electrophoresis and capillary electrophoresis (CE) became established analytical standards in numerous fields. A new era was brought by the 21st century with new insights to the field of electrokinetics; as major advances have been reported during the last 10 years on the strong-field theory, which is the realm of nonlinear electrokinetic phenomena.

The present review article is focused on the assessment, analysis, enrichment and sorting of synthetic particles and cells employing nonlinear electrokinetic methods. The assessment of particles and intact microorganisms is essential in numerous fields and applications, and nonlinear electrokinetic methods have proven to be an attractive option for providing rapid, robust, and portable tools to answer this need. This article is organized as follows: Section 1 contains this introduction which describes the general background and motivation of the present article. Sections two through four are focused on the fundamental theory and applications of electrorotation, dielectrophoresis and nonlinear electrophoresis, respectively. Section 5, the concluding remarks, offers a summary of the findings and reports described in this article and provide an outlook on expected future developments.

2. ELECTROROTATION

The use of rotating electric fields enables the employment of electrorotation for the characterization particles and cells (28). In particular, electrorotation has been used extensively as tool for assessing the viability and dielectric properties of cells (4).

2.1 Operating principle and target cell/particle characteristics probed

When a polarizable particle, immersed in an electrolyte solution, is exposed to an external electric field, the charges in the electrical double layer (EDL) around the particle (also called bulk charge) experience a force that causes them to move around the particle towards the electrode of the opposite charge (3). Then, the charges accumulate at the interface between the electrolyte and the particle, causing a charge imbalance in the particle and producing an induced dipole moment. In a homogenous electric field, the dipole aligns with the electric field direction, but it takes a finite length of time for this alignment to occur. If rotating (phase-shifting) electric fields are employed, the induced dipole will continuously re-align itself with the electric field vector, resulting in a rotating asynchronous motion of the particle around its own axis. The expressions for the

electro-rotational torque (Γ_{EROT}) and angular velocity ($\Omega_{EROT(\omega)}$) of a spherical particle are:

$$\Gamma_{EROT} = -4\pi\varepsilon_m r_p^3 \text{Im}[f_{CM}] |\mathbf{E}|^2$$
 (1)

$$\mathbf{\Omega}_{EROT(\omega)} = -\frac{\varepsilon_m}{2\eta} \text{Im}[f_{CM}] |\mathbf{E}|^2$$
 (2)

where r_p is the particle diameter, ε_m and η are the medium electric permittivity and viscosity, respectively; ${\rm Im}[f_{CM}]$ is the imaginary part of the Clausius-Mossotti factor, and ${\bf E}$ is the electric field. The f_{CM} , defined as $f_{CM}=(\varepsilon_p^*-\varepsilon_m^*)/(\varepsilon_p^*-\varepsilon_m^*)$, accounts for the polarizability of the particle relative to that of the suspending medium, where the complex permittivity is defined as $\varepsilon^*=\varepsilon-j\sigma/\omega$, where ε and σ are the real permittivity and conductivity of the particle or media, and $j=\sqrt{-1}$ and ω is the frequency of the field (3, 29). Electrorotation probes the dielectric properties of the particles and the differences in polarizability between the particle and the media, which are observed in terms of the direction of the resulting particle rotation.

2.2 Example applications

Electrorotation has been mainly employed for characterization purposes. In cell analysis, electrorotation allows differentiating between distinct groups of cells by exploiting the differences in their dielectric properties. An important area for electrorotation has been cell viability assessments, as dead and live cells differ in their dielectric properties, resulting in distinct electrorotation responses (30). Electrorotation has been employed for the electrophysiological analysis of a wide range of cells, including bacteria (29, 31) mammalian cells (29, 32), and even parasites (33). The next two subsections describe recent applications of electrorotation for the assessment of synthetic particles and cells.

2.2.1 Particles

Some of the first applications of electrorotation for particle assessments were published in the field of physics (34–36). The first study on the measurement of the dielectric properties of latex particles was published in 1962 by Schwan et al. (34). A pioneering electrorotation report was the single particle rotation study by Arnold et al. (35). They used ten distinct types of polystyrene particles of three sizes (diameters of 5-6 μm, 9-10 μm and 46.5 μm). They employed both non-functionalized and carboxylated (COO-) particles and noticed that the surface treatment impacted the particles' electrorotation response. They measured the rotation spectrum (rotation rate in rad/s vs. electric field frequency) and the resulting spectra contained two "peaks," one peak at low frequencies and one peak at high frequencies. **Figure 1a** illustrates these results, where a partial first peak occurs at frequencies below 1 kHz. This peak is partial since no experiments were performed at frequencies below 100 Hz due to particles oscillations (which were attributed to electrophoretic effects). The second rotation peak occurs between 10-1000 kHz. Similar results were reported by Zhou et al. (37) with 6-μm polystyrene beads and Falokun and Markx (38) with 90-μm κ-carrageenan gel beads. Their results showed that both polystyrene and gel beads rotate in the co-field direction. Zhou et al. observed two peaks (37) while Falokun and Markx (38) observed only the high frequency peak, since they employed frequencies above 2 kHz.

Semiconductor materials have also been assessed with electrorotation and the Morgan and Ramos research groups have reported several studies (39-41). Recently they reported the electrorotation spectra of several different types of semiconducting materials including microparticles, ZnO nanowires, doped silicon and Su-8. Their results illustrated two distinct peaks in the electrorotation spectra of the semiconducting particles; at low frequencies particles rotated in the counterfield direction, while rotation in the cofield direction occurred at higher frequencies. The rotation response of ZnO semiconducting nanowires is included in Figure 1b which exhibits two rotation peaks, one in the counterfield and one in the cofield direction at low and high frequencies, respectively (40). This response is the result of the two distinct relaxation mechanisms that semiconducting particles experience: the charging of the EDL, which also occurs with metallic particles; and the Maxwell-Wagner relaxation caused by the differences in electrical properties between the particle and the suspending medium. These groups also studied the electrorotation spectra of metallic particles including titanium (42) and gold-coated (43) microparticles. The results obtained with gold particles are shown in Figure 1c, which for each type of particle only feature a single rotation velocity peak in the counterfield direction caused by the charging of the EDL (43). The rotation velocity, although plotted as "positive" in Figure 1c, illustrates counterfield rotation as all values of Ω_{EROT} are negative. These reports demonstrated that the electrorotation spectra allows for the determination of the dielectric properties of particles over the range of dielectric, semiconducting to conductive materials.

2.2.2 Cells

The analysis of cells, in particular cell viability assessments (30), is the area where electrorotation excels. Since electrorotation probes the dielectric properties of cells, it has been used extensively in combination with dielectrophoresis to assess cell membrane and cell cytoplasm characteristics (44, 45), including single-cell analysis (46) and cell-cell interactions (4). Electrorotation has been utilized for studying plant cells (47), bacteria (4, 29, 31, 48), bacterial aggregates (38) and biofilms (37), yeast (38, 49, 50), red blood cells (49, 51, 52), white blood cells (32, 49, 53), cancer cells (29, 32, 46, 49, 54), gametes and embryos (55), and parasites (33, 56). As electrorotation has been used broadly in cell analysis, the discussion here aims to provide the reader with an overview of the distinct applications of electrorotation.

Viability assessments is by far the most successful application of electrorotation and some of the early reports in the 1990s focused on viability determinations (30, 37, 38, 56–58). This technique is effective as a viability assessment tool because the electrorotation response of cells changes significantly when a cell dies. An excellent report published by Falokun and Markx (38) demonstrated how the electrorotation spectra changes from counterfield rotation to cofield rotation when a cells dies. These results, obtained with yeast cells, are shown in **Figure 2a-2b**. Their report (38) illustrated one of the most powerful applications of electrorotation as it allows for fast and label-free viability assessment of cells. Electrorotation viability assessments have also been performed with parasites (33, 56, 58) and bacterial cells (57).

As a non-invasive and label-free method, electrorotation has been used to determine changes in the electrical

properties of cells. Zhou et al. (50) used electrorotation for assessing the effect of Cosmocil (a biocide) on yeast cells. By analyzing the electrorotation spectra of the cells, before and after treatment, it was found that the cell membrane conductivity increased gradually with increasing concentrations of Cosmocil, revealing a progressive breakdown of the membrane. Voyer et al. (59) reported an improved approach for cell assessments with electrorotation by proposing the use of two sequential strategies: use of weight coefficients for the evaluation of electrorotation spectra, followed by the application of an optimization procedure (Nelder-Mead algorithm). The use of this approach increased the confidence level of the results. Two other recent electrorotation studies on determination of cells' properties were reported by Kawai et al. (45) and Lin et al. (49). In the former study (45) they characterized the membrane capacitance and cytoplasm conductivity of THP-1 cells, Jurkat cells and K265 cells employing a novel 3-dimensional interdigitated microelectrode array. In the later study (49), Lin et. al. analyzed the imaginary part of the CM factor, described in Equations (1-2), employing a system with planar electrodes stimulated at two distinct frequencies.

More recently, electrorotation has been applied for the characterization of a large variety of cancer cells, demonstrating the capabilities of this technique in clinical analysis. Trainito et al. (29) combined the use of negative dielectrophoresis and electrorotation methods to determine the dielectric properties of *E. coli*, Jurkat and human U87MG glioblastoma cells. The dielectrophoretic force allowed for trapping the cells on the surface of planar parabolic electrodes, then, the electrorotation spectra made it possible to determine the cells' dielectric properties. More recently, Trainito et al. (54) employed electrorotation to characterize three distinct stages of malignancy of mouse ovarian surface epithelial (MOSE) cells. These results are shown in **Figure 2c**, where it is observed how the cells' response changes with increasing malignancy. MOSE-E cells are the least malignant, while MOSE-L_{TICV} are the most malignant. The results showed that as tumor cells become more aggressive their morphology changes, as illustrated by an increase in membrane conductance and capacitance and cytoplasmic conductivity. These findings show the potential of electrorotation as a tool for the monitoring of cancer progression.

Keim et al. (32) also used electrorotation in a device with microcages to assess the dielectric properties of cancer cells. They studied HeLA, human embryonic kidney 293, and human immortalized T lymphocytes cells. Their results agreed with previously reported values, demonstrating electrorotation as robust method for assessing cell properties. Huang et al. published two recent reports (46, 53) on the measurement of the dielectric properties of cancer cells. In their most recent work (46) they studied HeLa, A549, HepaRG, MCF7, and MCF10A cells by combining optical stretching and electrorotation. Optical trapping and stretching allowed measuring mechanical properties, while electrorotation enabled measuring dielectric properties. The electrorotation spectra for these five cell types are shown in **Figure 2d** and a plot of cytoplasmic conductivity vs. membrane capacitance, which extracted from electrorotation data, is given in **Figure 2e**. These results demonstrate the applicability of electrorotation as a single-cell method for accurate characterization of cancer cells.

3. DIELECTROPHORESIS

Dielectrophoresis, a phenomenon that depends on particle polarization, has been used extensively for the manipulation of a wide range of particles across scales, ranging from molecules to parasites (14, 44, 60).

3.1 Operating principle and target cell/particle characteristics probed

Dielectrophoresis, a nonlinear electrokinetic phenomenon, is the resulting particle motion due to polarization effects under the influence of a nonuniform electric field. The expressions for the dielectrophoretic force and velocity on a spherical particle are:

$$\mathbf{F}_{DEP} = 2\pi r_p^3 \varepsilon_m \operatorname{Re}[f_{CM}] \nabla E^2 \tag{3}$$

$$\mathbf{v}_{DEP} = \mu_{DEP} \nabla E^2 = \frac{r_p^2 \varepsilon_m}{3n} \operatorname{Re}[f_{CM}] \nabla E^2$$
 (4)

where μ_{DEP} is the dielectrophoretic mobility, ∇E^2 represents the gradient of the squared electric field magnitude and $\text{Re}[f_{CM}]$ is the real part of the f_{CM} , which accounts for the particle polarizability with respect to that of the suspending media. Dielectrophoresis particle migration can be positive or negative. Positive dielectrophoresis is when the particle is more polarizable than the media and is attracted to the regions of higher field gradient and negative dielectrophoresis is the opposite, and the particle is repelled from these regions. The dielectrophoretic response of particles and cells depends greatly on the frequency of the electric field. This dependance allows probing distinct cellular properties, as well as subcellular regions, from the membrane to the cytoplasm properties.

3.2 Example applications

Dielectrophoresis was first observed in 1951 with carbon particles (61) in a rudimentary system in a petri dish. Since then, numerous reports have illustrated the manipulation, assessment, and separation of synthetic particles and bioparticles including macromolecules, cell organelles and microorganisms (5). The discussion below provides an overview of these applications.

3.2.1 Particles

Numerous studies have reported the dielectrophoresis-based manipulation and patterning of synthetic particles and bioparticles in microsystems (62–67). Significant efforts have been devoted to protein dielectrophoresis, as the effects of dielectrophoresis on proteins are still not fully understood. Excellent review articles on this technique have been published by Pethig and Holzel (68–70). In 2017 Mohamad et al. (71) reported the characterization of colloidal protein particles by employing impedance measurements. They developed a robust label-free strategy that made it possible to monitor the impedance of bovine serum albumin (BSA) protein particles as they collected between the microelectrodes in the device shown in **Figure 3a**. The novelty of this work was the observation of the two dispersion behaviors shown in **Figure 3b**. The first dispersion occurring at 400 kHz was attributed to the molecule's orientation towards the applied electric field,

while the second dispersion was identified as Maxwell-Wagner dispersion. The authors stated that their proposed approach could also be applied to DNA and other molecular scale objects. This study illustrated the potential of dielectrophoresis for the dielectric characterization of nano-sized particles, such as proteins. Other recent studies have focused on the use of dielectrophoresis for the rapid concentration of protein molecules in devices with insulating structures (72), and the shape-based isolation of protein particles in a device with circular traps (73). Carbon nanotubes (CNTs), cylindrical large molecules with important applications in numerous fields, have also been studied with dielectrophoresis. Most of the studies have focused on the patterning or probing the dielectric properties of these particles. Duchamp et al. (74) demonstrated their precise patterning onto microelectrodes by means of dielectrophoresis. They found that solvent and substrate characteristics had a strong effect on the dielectrophoresis-based patterning. A major application of patterned CNTs is for the fabrication of sensors as reported by Li et al. (75). They employed a dielectrophoresis-based method for the alignment of single-wall CNTs for the fabrication of a pH sensor. This approach used microelectrodes with a teeth-like geometry that enabled the accurate spatial deposition of the CNTs. The fabricated sensor showed good stability and high pH sensitivity with reproducible results, illustrating the potential applications of patterned CNTs. Similarly, An and Friedrich (76) investigated the dielectrophoresisassembly of CNTs. They determined that the uniformity in the length and stiffness of the nanotubes have a great influence on the stability and controllability of the resulting dielectrophoresis-based patterning. Probing the properties of CNTs is essential for selecting suitable nanotubes for desired applications.

Rabbani et al. (77) assessed the zeta potential (a surrogate for electrical charge) of single-wall CNTs wrapped in single-stranded DNA molecules. They employed an insulator-based dielectrophoresis (iDEP) system. This type of system employs either AC signals or DC-biased AC signals to enable dominant dielectrophoresis effects. Insulator-based systems stimulated with DC potentials are discussed in the next section. They employed an iDEP channel with cylindrical insulating posts stimulated with an AC potential. Their experimental findings, which agreed with mathematical modeling, showed that the DNA-wrapped CNTs exhibit both negative dielectrophoresis and positive dielectrophoresis as shown in **Figure 3c-3d**, respectively. Negative dielectrophoresis occurs when the CNTs are pushed outside these regions between the posts (**Fig. 3c**, sample A), while positive dielectrophoresis happens when the CNTs are trapped in these regions (**Fig. 3d**, sample B). The difference between sample A and B (which exhibited negative dielectrophoresis and positive dielectrophoresis, respectively), was the sonication time, 20 min for A and 60 min for B. The authors concluded that increasing the sonication time produces an increase on the zeta potential of the CNTs, altering their dielectric properties and dielectrophoretic response.

Dielectrophoresis has been proven to be effective for probing, separating and patterning many other types of particles, including nanowires (78, 79), nanoparticles (80–82) and microparticles (83–85). Weirauch et al. reported the material-based separation of microparticles employing an iDEP system stimulated with a DC-biased AC potential. **Figure 3e** illustrates the microchannel used in this study and **Figure 3f** depicts the

dielectropherogram of the separation of two populations of microparticles of the same size (2.4 µm polystyrene and 2.4 µm gold-coated polystyrene microparticles). The differences in the dielectric properties of the particle material enabled the separation. **Figure 3f**, depicts the fluorescence signal (electropherogram) obtained at the channel outlet as the particles eluted the post array along with the magnitude of the applied AC voltage, demonstrating the material-based separation. Other dielectrophoresis-based systems have demonstrated shape selective microparticle manipulation in filtration systems (85), additive manufacturing by manipulating liquid droplets (86), fouling suppression in bioreactors and for the mixing of submicron particles (87). These applications further demonstrate the potential of dielectrophoresis for the manipulation of a wider array of particles.

3.2.2 Cells

Cell analysis is perhaps the major application area of dielectrophoresis (44, 88, 89), as probing the dielectric properties of cells allows for label-free, robust and comprehensive cell assessments. Dielectrophoresis has been used to distinguish between live and dead cells (90–96), separate and characterize distinct cell types (95–100), and even assess cell capabilities in assisted reproductive technologies (55). As with dielectrophoresis of particles, there are numerous configurations of dielectrophoresis systems used with cells, including traditional dielectrophoresis with 2D planar electrodes (94, 95), 3D electrodes (92, 96), 3D dielectrophoresis wells (97–99), insulator-based dielectrophoresis (90, 91), isomotive dielectrophoresis (88) and traveling wave dielectrophoresis (100).

Distinguishing between live and dead cells is one of the most important capabilities of dielectrophoresis and many distinct systems have developed for cell viability assessments. The Agah research group reported a 3D-iDEP system that allowed for cell trapping and separation of live from dead bacterial cells at lower applied potentials than traditional 2D-iDEP systems (90, 91). Live and dead cell separations have also been achieved with 3D electrode-based dielectrophoresis devices. Yildizhan et al. (92) performed the selective trapping of live U937 monocytes from a sample containing live and dead monocytes by employing a 3D array of carbon electrodes stimulated with an AC potential. The live monocytes exhibited strong positive dielectrophoresis force while the dead ones exhibited almost no dielectrophoresis response, enabling successful live/dead cell differentiation. **Figure 4a** shows live and dead monocytes inside the device before voltage treatment while **Figure 4b** shows trapped live monocytes exhibit positive dielectrophoresis after voltage treatment upon removal of the dead monocytes. Sample loading and dead monocyte removal was achieved employing a flow rate of 1 µL/min. Some of the trapped live monocytes in **Figure 4b** are in peal-chain formations as indicated by the red arrows. These results illustrate that dielectrophoresis-based systems are robust platforms for live and cell discrimination.

Another major application area of dielectrophoresis, as with electrorotation, is the characterization of a cell's dielectric properties. There is a plethora of novel dielectrophoresis-based systems developed for cell characterization (44, 89). Some of these systems are now commercially available (101). An example of a

dielectrophoresis commercially available platform is the 3D dielectrophoresis system by DEPtech (97–99). The chip, shown in **Figure 4c**, contains 20 distinct wells that operate at different frequencies, as depicted in **Figure 4d**. This makes it possible to collect 20 distinct data points (dielectrophoretic response vs. frequency) to build the dielectrophoretic spectra for cell characterization. The walls of the wells contain the electrodes. Cells exhibiting negative dielectrophoresis are repelled by the electrodes towards the center of the well and cells exhibiting positive dielectrophoresis are attracted towards the wall and trapped by the electrodes. Since the f_{CM} depends on frequency, the dielectrophoretic response of the cells can vary in magnitude and direction, from negative dielectrophoresis to positive dielectrophoresis. **Figure 4e** illustrates negative dielectrophoresis and positive dielectrophoresis cell behavior, obtained at two distinct frequencies (98). This system was used for assessing the efficacy of chemotherapy and radiotherapy on two distinct cancer cell lines (from neck and head carcinoma). The 3D dielectrophoresis platform allowed identifying changes in the cells' dielectric characteristics after anticancer treatment. More recently, this group developed a rapid cell electrophysiology evaluation system with an impressive 100 data point DEP spectra acquisition in less than two minutes. They were able to characterize several cell types, ranging from platelets to cardiac cells employing the system in **Figures 4c-4e**.

Separation and sorting of samples containing mixtures of cells is a major need in cell analysis. The 3D dielectrophoresis system has also been employed for effective cell enrichment of binary mixtures of cells, including yeast, red blood cells (RBC) and cancer cells (97). Insulator-based dielectrophoresis systems, due to their simplicity, are a popular platform for cell separation and sorting. These include contactless dielectrophoresis systems (102), 3D iDEP microchannels (103), packed beds configurations (93) and hybrid electrode and iDEP platforms (104). Other popular configurations for dielectrophoresis-based cell sorting and separation are complementary metal-oxide-semiconductor devices that employ electrodes to exert dielectrophoresis forces on cells (94, 95).

4. NONLINEAR ELECTROPHORESIS

This section refers to systems where nonlinear electrophoresis is a major, if not the dominant, force influencing particle migration and manipulation. The systems covered in this section are insulator-based electrokinetic (iEK) devices that are stimulated with DC potentials or low frequency AC potentials; thus, electrophoretic effects are not cancelled out (26, 105).

4.1 Operating principle and target cell/particle characteristics probed

In iEK systems, there is a combination of linear and nonlinear phenomena that influence the overall particle migration and behavior. The linear phenomena are linear electrophoresis (EP_L) and electroosmosis (EO), whose velocities are described as:

$$\mathbf{v}_{EP,L} = \mu_{EP,L} \mathbf{E} = \frac{\varepsilon_m \zeta_P}{n} \mathbf{E}$$
 (5)

$$\mathbf{v}_{EO} = \mu_{EO} \mathbf{E} = -\frac{\varepsilon_m \zeta_W}{n} \mathbf{E}$$
 (6)

where $\mathbf{v}_{EP,L}$ refers to the linear electrophoretic velocity and \mathbf{v}_{EO} represent the linear EO velocity, and ζ is the zeta potential of the particle or the channel wall. The notation "L" in the linear electrophoretic velocity (and mobility) is used to distinguish it from the nonlinear electrophoretic velocity ($\mathbf{v}_{EP,NL}$).

The nonlinear phenomena present in iEK systems are dielectrophoresis as described in Eqn. (4), and nonlinear electrophoresis for which the following expressions have been developed for the two limiting cases of the Peclet number of $Pe \ll 1$ and $Pe \gg 1$. There are no analytical expressions yet for intermediate values of Peclet number. In these expressions the velocity of nonlinear electrophoresis can have either a cubic or a 3/2 dependance with the electric field, as shown below:

$$\mathbf{v}_{EP,NL}^{(3)} = \mu_{EP,NL}^{(3)} \mathbf{E}^3$$
 for arbitrary Du and $Pe \ll 1$

$$\mathbf{v}_{EP,NL}^{(3/2)} = \mu_{EP,NL}^{(3/2)} \mathbf{E}^{3/2}$$
 for $Du \ll 1$ and $Pe \gg 1$

where $\mu_{EP,NL}^{(n)}$ denotes the mobility of nonlinear electrophoresis (EP_{NL}) with an electric filed dependance of n (where n=3 or n=3/2), and Du is the Dukhin number. The $\mathbf{v}_{EP,NL}^{(n)}$ depends on \mathbf{E}^n and the value of $\mu_{EP,NL}^{(n)}$, which in turn depends on the bulk charge of the particle or cell. Recent publications have focused on the experimental characterization of $\mu_{EP,NL}^{(n)}$ of particles and cells (8, 64, 106–108). In iEK systems, the overall particle velocity depends on four electrokinetic phenomena listed above (Eqns. (4-8)):

$$\mathbf{v}_P = \mathbf{v}_{EO} + \mathbf{v}_{EP,L} + \mathbf{v}_{DEP} + \mathbf{v}_{EP,NL}^{(n)}$$
(9)

Since the $\mu_{EP,NL}^{(n)}$ depends on particle shape and size (27), EP_{NL} has the valuable capability of being able to discriminate particles by their shape or size, a discrimination that is not possible under purely linear electrophoresis (109).

4.2 Example applications

This section discusses recent iEK systems employed for particle and cell manipulation. In the past, many of these systems had been labeled iDEP since it was believed that dielectrophoresis was the dominant electrokinetic phenomena. However, recent developments (110–112) have unveiled that in iEK platforms stimulated with DC or low-frequency AC potentials, dielectrophoresis is not the dominant electrokinetic phenomenon (113), and instead EP_{NL} is a major effect that can dominate particle migration under high electric fields (26, 105, 114).

4.2.1 Particles

Although nonlinear electrophoresis is not a new topic, as it first was reported by Dukhin and collaborators in the early 1970s (115), its development as analytical and particle manipulation technique is somewhat recent. A main challenge for the broad development of EP_{NL} was the lack of experimental data to support the already

existing theoretical models (116). Major advances on EP_{NL} have been reported during the last decade (27), as our understanding of particle behavior outside the weak-field regime continues to grow.

There are numerous reports on particle manipulation in systems labelled as DC-iDEP (117), however, recent developments have revealed that dielectrophoresis is not the dominant effect in these systems, actually dielectrophoresis is a minor effect (113). Particle overall migration is the result of several electrokinetic effects as illustrated in Eqn. (9), where EP_{NL} can be dominant and enable particle trapping at high electric fields (110). By properly accounting for the effects of EP_{NL} on particle migration, it has been possible to separate highly similar particles and to obtain much better agreement between experimental data and modeling results (118). Prior to considering EP_{NL} in mathematical models of iEK systems, it was necessary to add correction factors to these previous models to achieve agreements with experimental results (119).

Recent reports illustrated that EP_{NL} strongly affects the magnitude and direction of particle migration in a simple microchannel under a DC electric field, and can even cause particle trapping and reversal migration at high electric fields (110-112). Figure 5a shows the characterization of particle velocity as a function of the electric field (E) for three types of negatively charged (negative ζ_P) polystyrene particles in a microchannel made from PDMS (negative ζ_W) reported by Cardenas-Benitez (110). All three distinct types of particles exhibit the same behavior, which can be divided into three stages. First, the overall velocity increases linearly with E, second, the velocity reaches a maximum as EP_{NL} effects are becoming significant, and third, particle velocity decreases with increasing E and even becomes negative (particle reversal) as EP_{NL} becomes the dominant phenomenon. It is important to note that dielectrophoretic effects are not seen in Figure 5a, as the electric field has a uniform distribution and dielectrophoresis requires electric field gradients. By characterizing the mobility of EP_{NL} of each particle and including it in mathematical models, Vaghef-Koodehi et al. (118) designed the separation of two highly similar particles as shown in Figure 5b. A simple four-reservoir microchannel with asymmetric insulating posts was used to separate a binary mixture of particles that had the same size (5.1 µm diameter), same shape and were made from the same substrate material. These two distinct types of particles only differed slightly in the magnitude of their negative electrical charge, as they had a difference in ζ_P of 3.4 mV. The overall migration of the particles was influenced by the four electrokinetic phenomena included in Eqn. (9). The image of the particles migrating across the insulating post array clearly show the red particles ($\zeta_P = -27.2 \ mV$) migrating ahead of the green particles ($\zeta_P = -30.8 \ mV$). The electropherogram with a resolution of Rs = 1.14 illustrates the separation, although not complete (since Rs <1.5), is encouraging since the particles had almost identical chemical and physical characteristics. Thanks to the inclusion of EP_{NL} in the model, the modeling results in this study were in good agreement with experimental results, without the use of any correction factors. These results illustrate the potential of employing EP_{NL} for separating target particles with similar characteristics.

4.2.2 Cells

Nonlinear electrophoresis has been successfully used for the assessment and manipulation of cells, however, many of these studies had been labelled as DC-iDEP systems (60, 120), when in reality it was EP_{NL}, instead of dielectrophoresis that was the main phenomenon responsible for cell trapping and enrichment (26, 105). There is a plethora of excellent studies using EP_{NL} for cell viability assessments (121, 122), separation, sorting and identification of cell mixtures (123–127), and the characterization of cells' dielectric properties (128–132). However, since it was very recently unveiled that EP_{NL} is a major force present in iEK systems (110–112), there are not many reports that discuss cell manipulation in terms of EP_{NL}. All the reports cited above discuss their findings in terms of dielectrophoresis. Detailed discussions of EP_{NL} vs. iDEP can be found here (26, 105, 114).

The effects of EP_{NL} in DC-iEK systems have recently been identified and characterized by several groups (64, 106–108, 110–112). The characterization of $\mu_{EP,NL}^{(n)}$ of cells (bacteria and yeast) was recently reported by Antunez-Vela at al. (107) employing a similar microchannel to the one shown in Figure 5a. The results are consistent with those obtained by Cardenas-Benitez (110) with polystyrene microparticles. As seen in Figure 6a the overall velocity of cells as a function of E follows the same three stages: i) linear increase with E, ii) reach a velocity maximum, and iii) decrease as E continues to increase reaching negative values (velocity reversal). By considering EP_{NL} in mathematical models of iEK systems, Vaghef-Koodehi et al. (8) was able to design effective DC-iEK systems to separate binary samples of distinct types of cells. Shown in Figures 6b-6c are two separate electropherograms of closely related cell types carried out in the same four-reservoir microchannel illustrated in Figure 5b. The first electropherogram (Fig. 6b) shows the separation of Saccharomyces cerevisiae and Escherichia coli cells, where two separated peaks are observed with a Rs = 2.13, where the green peak corresponds to E. coli cells. The second electropherogram (Fig. 6c) corresponds to the separation between Bacillus cereus and S. cerevisiae cells with Rs = 3.52, where the red peak corresponds to S. cerevisiae cells. The green peak in this second separation is wide, probably due to a higher population distribution (cell population heterogeneity) for B. cereus. The retention time of the cells in these separations were predicted with a COMSOL model and good agreement between modeling and experimental results was obtained. The application of DC-iEK systems allows shifting the separation process from linear to no linear electrokinetic regimes, by simply varying the magnitude of the electric field, since EP_{NL} effects become significant at higher electric fields. Furthermore, as the mobility of EP_{NL} depends on the size and shape of the particle/cell (27), employing EP_{NL} enables separations by exploiting cell size and shape differences, which are not possible with under purely linear electrophoresis conditions (109).

5. CONCLUSION AND FUTURE TRENDS

Nonlinear electrokinetic methods have been proven as successful methodologies for the analysis and separation of synthetic particles and cells. Employing electrokinetic methods enables the development of

label-free, robust and portable microfluidic platforms for the assessment of a wide variety of microparticles and cells. The reports reviewed and discussed in this article, which cover the electrokinetic phenomena of electrorotation, dielectrophoresis and EP_{NL}, describe the distinct particle/cell characteristics that can be exploited to achieve a successful and separation processes. The field of nonlinear electrokinetic is continuously evolving and new approaches and developments are making it possible to design highly discriminatory assessments for complex biological samples. There is still plenty to be learned in the dynamic field of nonlinear electrokinetic, and as predicted by Khair (27), the 21st century will bring a plethora of new developments that will further expand our understanding of nonlinear electrokinetic phenomena and enable new and existing applications making possible separations that were otherwise not feasible with traditional linear electrokinetic phenomena.

DISCLOSURE STATEMENT

The author is not aware of any affiliations, memberships, funding, or financial holdings that might be perceived as affecting the objectivity of this review.

ACKNOWLEDGMENT

The author gratefully acknowledges the National Science Foundation (Awards CBET-2127592 and CBET-2133207) for financial support.

LITERATURE CITED

- 1. Hughes MP. 2002. Nanoelectromechanics in engineering and biology. Boca Raton, FL: CRC Press.1st ed.
- 2. Jones TB. 1995. *Electromechanics of Particles*. New York, USA: Cambridge University Press.
- 3. Hywel M, Green NG. 2003. *AC Electrokinetics: Colloids and Nanoparticles Microtechnologies and microsystems series*. Baldock, Hertfordshire, UK: Research Studies Press.
- 4. Sancho M, Martínez G, Muñoz S, Sebastián JL, Pethig R. 2010. Interaction between cells in dielectrophoresis and electrorotation experiments. *Biomicrofluidics*. 4(2):022802
- 5. Kim D, Sonker M, Ros A. 2019. Dielectrophoresis: From Molecular to Micrometer-Scale Analytes. *Anal. Chem.* 91(1):277–95
- 6. Han CH, Woo SY, Bhardwaj J, Sharma A, Jang J. 2018. Rapid and selective concentration of bacteria, viruses, and proteins using alternating current signal superimposition on two coplanar electrodes. *Sci. Rep.* 8(1):14942
- Hilton SH, Crowther C V., McLaren A, Smithers JP, Hayes MA. 2020. Biophysical differentiation of susceptibility and chemical differences in Staphylococcus aureus. *Analyst.* 145(8):2904–14
- 8. Vaghef-Koodehi A, Ernst OD, Lapizco-Encinas BH. 2023. Separation of Cells and Microparticles in Insulator-Based Electrokinetic Systems. *Anal. Chem.* 95(2):1409–18
- 9. Su Y-HH, Tsegaye M, Varhue W, Liao K-TT, Abebe LS, et al. 2014. Quantitative dielectrophoretic tracking for characterization and separation of persistent subpopulations of Cryptosporidium parvum. *Analyst.* 139(1):66–73

- Keck D, Stuart C, Duncan J, Gullette E, Martinez-Duarte R. 2020. Highly Localized Enrichment of Trypanosoma brucei Parasites Using Dielectrophoresis. *Micromachines*. 11(6):625
- Chuang HS, Raizen DM, Lamb A, Dabbish N, Bau HH. 2011. Dielectrophoresis of Caenorhabditis elegans. *Lab Chip*. 11(4):599–604
- 12. Shokouhmand H, Abdollahi A. 2020. Detection of cell-free DNA nanoparticles in insulator based dielectrophoresis systems. *J. Chromatogr. A.* 1626:461262
- 13. Gudagunti FD, Velmanickam L, Nawarathna D, Lima IT. 2020. Nucleotide identification in DNA using dielectrophoresis spectroscopy. *Micromachines*. 11(1):39
- 14. Lapizco-Encinas BH. 2020. Microscale electrokinetic assessments of proteins employing insulating structures. *Curr. Opin. Chem. Eng.* 29:9–16
- 15. Vaghef-Koodehi A, Lapizco-Encinas BH. 2022. Microscale electrokinetic-based analysis of intact cells and viruses. *Electrophoresis*. 43(1–2):263–87
- 16. Ermolina I, Milner J, Morgan H. 2006. Dielectrophoretic investigation of plant virus particles: Cow Pea Mosaic Virus and Tobacco Mosaic Virus. *Electrophoresis*. 27(20):3939–48
- 17. Masuda T, Maruyama H, Honda A, Arai F. 2014. Virus enrichment for single virus infection by using 3D insulator based dielectrophoresis. *PLoS One*. 9(6):e94083
- Coll De Peña A, Mohd Redzuan NH, Abajorga M, Hill N, Thomas JA, Lapizco-Encinas BH. 2019. Analysis of bacteriophages with insulator-based dielectrophoresis. *Micromachines*. 10(7):450
- Nowicka AB, Czaplicka M, Szymborski T, Kamińska A. 2021. Combined negative dielectrophoresis with a flexible SERS platform as a novel strategy for rapid detection and identification of bacteria. *Anal. Bioanal. Chem.* 213(7):2007–20
- Ringwelski B, Jayasooriya V, Nawarathna D. 2020. Dielectrophoretic High Purity Isolation of Primary T-cells in Samples Contaminated with Leukemia Cells, for Biomanufacturing of Therapeutic CAR T-cells. *J. Phys. D.* Appl. Phys. 54(6):10
- Nguyen NV, Jen CP. 2018. Impedance detection integrated with dielectrophoresis enrichment platform for lung circulating tumor cells in a microfluidic channel. *Biosens. Bioelectron.* 121:10–18
- 22. Jun S, Chun C, Ho K, Li Y. 2021. Design and evaluation of a millifluidic insulator-based dielectrophoresis (Dep) retention device to separate bacteria from tap water. *Water (Switzerland)*. 13(12):1678
- 23. Du F, Hawari AH, Larbi B, Ltaief A, Pesch GR, et al. 2018. Fouling suppression in submerged membrane bioreactors by obstacle dielectrophoresis. *J. Memb. Sci.* 549(October 2017):466–73
- 24. Choi W, Min YW, Lee KY, Jun S, Lee HG. 2020. Dielectrophoresis-based microwire biosensor for rapid detection of Escherichia coli K-12 in ground beef. *LWT Food Sci. Technol.* 132:109230
- 25. Mishchuk NA, Takhistov P V. 1995. Electroosmosis of the second kind. *Colloids Surfaces A Physicochem. Eng. Asp.* 95(2–3):119–31
- Lapizco-Encinas BH. 2022. The latest advances on nonlinear insulator-based electrokinetic microsystems under direct current and low-frequency alternating current fields: a review. *Anal. Bioanal. Chem.* 414(2):885-905
- 27. Khair AS. 2022. Nonlinear electrophoresis of colloidal particles. Curr. Opin. Colloid Interface Sci. 59:101587

- 28. Pethig R. 2017. *Dielectrophoresis: theory, methodology, and biological applications*. Chichester, West Sussex, UK: John Wiley & Sons.
- 29. Trainito CI, Bayart E, Bisceglia E, Subra F, Français O, Le Pioufle B. 2016. Electrorotation as a versatile tool to estimate dielectric properties of multi-scale biological samples: From single cell to spheroid analysis. *IFMBE Proceedings*, 53:75–78
- 30. Patel P, Markx GH. 2008. Dielectric measurement of cell death. Enzyme Microb Technol. 43(7):463-70
- 31. Holzel R. 1999. Non-invasive determination of bacterial single cell properties by electrorotation. *Biochim. Biophys. Acta Mol. Cell Res.* 1450(1):53–60
- 32. Keim K, Rashed MZ, Kilchenmann SC, Delattre A, Gonçalves AF, et al. 2019. On-chip technology for single-cell arraying, electrorotation-based analysis and selective release. *Electrophoresis*. 40(14):1830–38
- 33. Dalton C, Goater AD, Burt JPH, Smith H V. 2004. Analysis of parasites by electrorotation. *Journal of Applied Microbiology*, 96(1):24–32
- 34. Schwan HP, Schwarz G, Maczuk J, Pauly H. 1962. On the low-frequency dielectric dispersion of colloidal particles in electrolyte solution. *J. Phys. Chem.* 66(12):2626–35
- 35. Arnold WM, Schwan HP, Zimmermann U. 1987. Surface conductance and other properties of latex particles measured by electrorotation. *J. Phys. Chem.* 91(19):5093–98
- Washizu M, Jones TB. 1996. Generalized multipolar dielectrophoretic force and electrorotational torque calculation. J. Electrostat. 38(3):199–211
- 37. Zhou X-FXF, Markx GH, Pethig R, Eastwood IM. 1995. Differentiation of viable and non-viable bacterial biofilms using electrorotation. *Biochim. Biophys. Acta Gen. Subj.* 1245(1):85–93
- 38. Falokun CD, Markx GH. 2007. Electrorotation of beads of immobilized cells. J. Electrostat. 65(7):475-82
- 39. García-Sánchez P, Flores-Mena JE, Ramos A. 2019. Modeling the AC electrokinetic behavior of semiconducting spheres. *Micromachines*. 10(2):100
- 40. García-Sánchez P, Ramos A. 2017. Electrorotation and Electroorientation of Semiconductor Nanowires. *Langmuir*. 33(34):8553–61
- 41. Morganti D, Morgan H. 2011. Characterization of non-spherical polymer particles by combined electrorotation and electroorientation. *Colloids Surfaces A Physicochem. Eng. Asp.* 376(1–3):67–71
- 42. Arcenegui JJ, Ramos A, García-Sánchez P, Morgan H. 2013. Electrorotation of titanium microspheres. *Electrophoresis*. 34(7):979–86
- 43. Ren YK, Morganti D, Jiang HY, Ramos A, Morgan H. 2011. Electrorotation of metallic microspheres. *Langmuir*. 27(6):2128–31
- 44. Lapizco-Encinas BH. 2021. Microscale nonlinear electrokinetics for the analysis of cellular materials in clinical applications: a review. *Microchim. Acta.* 188(3):104
- 45. Kawai S, Suzuki M, Arimoto S, Korenaga T, Yasukawa T. 2020. Determination of membrane capacitance and cytoplasm conductivity by simultaneous electrorotation. *Analyst*. 145(12):4188–95
- 46. Huang L, Liang F, Feng Y, Zhao P, Wang W. 2020. On-chip integrated optical stretching and electrorotation enabling single-cell biophysical analysis. *Microsystems Nanoeng*. 6(1):57

- 47. Falokun CD, Mavituna F, Markx GH. 2003. AC electrokinetic characterisation and separation of cells with high and low embryogenic potential in suspension cultures of carrot (Daucus carota). *Plant Cell. Tissue Organ Cult.* 75(3):261–72
- 48. Rohani A, Moore JH, Su YH, Stagnaro V, Warren C, Swami NS. 2018. Single-cell electro-phenotyping for rapid assessment of Clostridium difficile heterogeneity under vancomycin treatment at sub-MIC (minimum inhibitory concentration) levels. *Sensors Actuators B Chem.* 276:472–80
- 49. Lin YY, Lo YJ, Lei U. 2020. Measurement of the imaginary part of the clausius-mossotti factor of particle/cell via dual frequency electrorotation. *Micromachines*. 11(3):329
- 50. Zhou XF, Markx GH, Pethig R. 1996. Effect of biocide concentration on electrorotation spectra of yeast cells. *Biochim. Biophys. Acta - Biomembr.* 1281(1):60–64
- 51. Georgieva R, Neu B, Shilov VM, Knippel E, Budde A, et al. 1998. Low frequency electrorotation of fixed red blood cells. *Biophys. J.* 74(4):2114–20
- 52. Gascoyne P, Pethig R, Satayavivad J, Becker FF, Ruchirawat M. 1997. Dielectrophoretic detection of changes in erythrocyte membranes following malarial infection. *Biochim. Biophys. Acta Biomembr.* 1323(2):240–52
- 53. Huang L, Zhao P, Wang W. 2018. 3D cell electrorotation and imaging for measuring multiple cellular biophysical properties. *Lab Chip*. 18(16):2359–68
- 54. Trainito CI, Sweeney DC, Čemažar J, Schmelz EM, Français O, et al. 2019. Characterization of sequentially-staged cancer cells using electrorotation. *PLoS One*. 14(9):e0222289
- 55. Karcz A, Van Soom A, Smits K, Verplancke R, Van Vlierberghe S, Vanfleteren J. 2022. Electrically-driven handling of gametes and embryos: taking a step towards the future of ARTs. *Lab on a Chip*, 22(10):1852–75
- 56. Dalton C, Goater AD, Drysdale J, Pethig R. 2001. Parasite viability by electrorotation. *Colloids Surfaces A Physicochem. Eng. Asp.* 195(1–3):263–68
- 57. Hodgson CE, Pethig R, Hanley QS, Earle CW, Pennebaker FM, et al. 1998. Determination of the viability of Escherichia coli at the single organism level by electrorotation. *Clin. Chem.* 44(9):2049–51
- 58. Dalton C, Goater AD, Pethig R, Smith H V. 2001. Viability of Giardia intestinalis cysts and viability and sporulation state of Cyclospora cayetanensis oocysts determined by Electrorotation. *Appl. Environ. Microbiol.* 67(2):586–90
- 59. Voyer D, Frénéa-Robin M, Buret F, Nicolas L. 2010. Improvements in the extraction of cell electric properties from their electrorotation spectrum. *Bioelectrochemistry*. 79(1):25–30
- 60. Hakim KS, Lapizco-Encinas BH. 2021. Analysis of microorganisms with nonlinear electrokinetic microsystems. *Electrophoresis*. 42(5):588–604
- 61. Pohl HA. 1951. The Motion and Precipitation of Suspensoids in Divergent Electric Fields. *J. Appl. Phys.* 22(7):869–71
- 62. Chen Q, Yuan YJ. 2019. A review of polystyrene bead manipulation by dielectrophoresis. *RSC Adv.* 9(9):4963–81
- 63. Pethig R. 2017. Review—Where Is Dielectrophoresis (DEP) Going? J. Electrochem. Soc. 164(5):B3049–55
- 64. Ernst OD, Vaghef-Koodehi A, Dillis C, Lomeli-Martin A, Lapizco-Encinas BH. 2023. Dependence of Nonlinear

- Electrophoresis on Particle Size and Electrical Charge. Anal. Chem. 95(16):6595-602
- 65. Lomeli-Martin A, Ahamed N, Abhyankar V V., Lapizco-Encinas BH. 2023. Electropatterning—Contemporary developments for selective particle arrangements employing electrokinetics. *Electrophoresis*, 44(11–12):884–909
- Modarres P, Tabrizian M. 2017. Alternating current dielectrophoresis of biomacromolecules: The interplay of electrokinetic effects. Sensors Actuators B Chem. 252:391–408
- 67. Pesch GR, Du F. 2021. A review of dielectrophoretic separation and classification of non-biological particles. *Electrophoresis*. 42(1–2):134–52
- 68. Pethig R. 2019. Limitations of the Clausius-Mossotti function used in dielectrophoresis and electrical impedance studies of biomacromolecules. *Electrophoresis*. 40(18–19):2575–83
- Hölzel R, Pethig R. 2020. Protein Dielectrophoresis: I. Status of Experiments and an Empirical Theory. *Micromachines*. 11(5):533
- Hölzel R, Pethig R. 2021. Protein dielectrophoresis: Key dielectric parameters and evolving theory. *Electrophoresis*. 42(5):513–38
- 71. Mohamad AS, Hamzah R, Hoettges KF, Hughes MP. 2017. A dielectrophoresis-impedance method for protein detection and analysis. *AIP Adv.* 7(1):015202
- 72. Zhang P, Liu Y. 2017. DC biased low-frequency insulating constriction dielectrophoresis for protein biomolecules concentration. *Biofabrication*. 9(4):45003
- 73. Kwak TJ, Jung H, Allen BD, Demirel MC, Chang WJ. 2021. Dielectrophoretic separation of randomly shaped protein particles. *Sep. Purif. Technol.* 262:118280
- 74. Duchamp M, Lee K, Dwir B, Seo JW, Kapon E, et al. 2010. Controlled positioning of carbon nanotubes by dielectrophoresis: Insights into the solvent and substrate role. *ACS Nano*. 4(1):279–84
- 75. Li P, Martin CM, Yeung KK, Xue W. 2011. Dielectrophoresis Aligned Single-Walled Carbon Nanotubes as pH Sensors. *Biosensors*. 1(1):23–35
- 76. An L, Friedrich C. 2013. Dielectrophoretic assembly of carbon nanotubes and stability analysis. *Prog. Nat. Sci. Mater. Int.* 23(4):367–73
- 77. Rabbani MT, Schmidt CF, Ros A. 2017. Single-Walled Carbon Nanotubes Probed with Insulator-Based Dielectrophoresis. *Anal. Chem.* 89(24):13235–44
- 78. Garciá Núez C, Braa AF, López N, Pau JL, Garciá BJ. 2020. Single GaAs nanowire based photodetector fabricated by dielectrophoresis. *Nanotechnology*. 31(22):225604
- Chang B, Zhao D. 2021. Direct assembly of nanowires by electron beam-induced dielectrophoresis.
 Nanotechnology. 32(41):415602
- 80. Kuzyk A. 2011. Dielectrophoresis at the nanoscale. *Electrophoresis*. 32(17):2307–13
- 81. Gierhart BC, Howitt DG, Chen SJ, Smith RL, Collins SD. 2007. Frequency dependence of gold nanoparticle superassembly by dielectrophoresis. *Langmuir*. 23(24):12450–56
- 82. Riahifar R, Marzbanrad E, Raissi B, Zamani C, Kazemzad M, Aghaei A. 2011. Sorting ZnO particles of different shapes with low frequency AC electric fields. *Mater. Lett.* 65(4):632–35

- 83. Zhao K, Li D. 2017. Continuous separation of nanoparticles by type via localized DC-dielectrophoresis using asymmetric nano-orifice in pressure-driven flow. *Sensors Actuators B Chem.* 250:274–84
- 84. Weirauch L, Lorenz M, Hill N, Lapizco-Encinas BH, Baune M, et al. 2019. Material-selective separation of mixed microparticles via insulator-based dielectrophoresis. *Biomicrofluidics*. 13(6):064112
- 85. Weirauch L, Giesler J, Baune M, Pesch GR, Thöming J. 2022. Shape-selective remobilization of microparticles in a mesh-based DEP filter at high throughput. *Sep. Purif. Technol.* 300:121792
- Duncan JL, Barlow Z, Schultz J, Davalos R V. 2022. Introducing Electric Field Fabrication: A Method of Additive Manufacturing Via Liquid Dielectrophoresis. SSRN Electron. J. 4:100107
- 87. Salmanzadeh A, Shafiee H, Davalos R V., Stremler MA. 2011. Microfluidic mixing using contactless dielectrophoresis. *Electrophoresis*. 32(18):2569–78
- 88. Rashed MZ, Williams SJ. 2020. Advances and applications of isomotive dielectrophoresis for cell analysis. *Anal. Bioanal. Chem.* 412(16):3813–33
- 89. Henslee EA. 2020. Review: Dielectrophoresis in cell characterization. *Electrophoresis*. 41(21–22):1915–30
- 90. Zellner P, Shake T, Hosseini Y, Nakidde D, Riquelme M V., et al. 2015. 3D Insulator-based dielectrophoresis using DC-biased, AC electric fields for selective bacterial trapping. *Electrophoresis*. 36(2):277–83
- 91. Nakidde D, Zellner P, Alemi MM, Shake T, Hosseini Y, et al. 2015. Three dimensional passivated-electrode insulator-based dielectrophoresis. *Biomicrofluidics*. 9(1):14125
- 92. Yildizhan Y, Erdem N, Islam M, Martinez-Duarte R, Elitas M. 2017. Dielectrophoretic separation of live and dead monocytes using 3D carbon-electrodes. *Sensors*. 17(11):2691
- 93. Lewpiriyawong N, Xu G, Yang C. 2018. Enhanced cell trapping throughput using DC-biased AC electric field in a dielectrophoresis-based fluidic device with densely packed silica beads. *Electrophoresis*. 39(5–6):878–86
- 94. Ettehad HM, Zarrin PS, Hölzel R, Wenger C. 2020. Dielectrophoretic immobilization of yeast cells using CMOS integrated microfluidics. *Micromachines*. 11(5):501
- 95. Ettehad HM, Wenger C. 2021. Characterization and separation of live and dead yeast cells using cmos-based dep microfluidics. *Micromachines*. 12(3):270
- 96. Nie X, Luo Y, Shen P, Han C, Yu D, Xing X. 2021. High-throughput dielectrophoretic cell sorting assisted by cell sliding on scalable electrode tracks made of conducting-PDMS. *Sensors Actuators B Chem.* 327:128873
- 97. Faraghat SA, Hoettges KF, Steinbach MK, van der Veen DR, Brackenbury WJ, et al. 2017. High-throughput, low-loss, low-cost, and label-free cell separation using electrophysiology-activated cell enrichment. *Proc. Natl. Acad. Sci.* 114(18):4591–96
- 98. Hoettges KF, Henslee EA, Torcal Serrano RM, Jabr RI, Abdallat RG, et al. 2019. Ten–Second Electrophysiology: Evaluation of the 3DEP Platform for high-speed, high-accuracy cell analysis. *Sci. Rep.* 9(1): 19153
- Mahabadi S, Labeed FH, Hughes MP. 2018. Dielectrophoretic analysis of treated cancer cells for rapid assessment of treatment efficacy. *Electrophoresis*. 39(8):1104–10
- 100. Varmazyari V, Ghafoorifard H, Habibiyan H, Ebrahimi M, Ghafouri-Fard S. 2022. A microfluidic device for label-free separation sensitivity enhancement of circulating tumor cells of various and similar size. *J. Mol. Liq.*

- 349:118192
- 101. Hughes MP. 2018. Technological developments in dielectrophoresis and its path to commercialization. *Cell Gene Ther. Insights.* 4(1):81–88
- 102. Salahi A, Varhue WB, Farmehini V, Hyler AR, Schmelz EM, et al. 2020. Self-aligned microfluidic contactless dielectrophoresis device fabricated by single-layer imprinting on cyclic olefin copolymer. *Anal. Bioanal. Chem.* 412(16):3881–89
- 103. Aghaamoo M, Aghilinejad A, Chen X, Xu J. 2019. On the design of deterministic dielectrophoresis for continuous separation of circulating tumor cells from peripheral blood cells. *Electrophoresis*. 40(10):1486–93
- 104. Torres-Castro K, Honrado C, Varhue WB, Farmehini V, Swami NS. 2020. High-throughput dynamical analysis of dielectrophoretic frequency dispersion of single cells based on deflected flow streamlines. *Anal. Bioanal. Chem.* 412(16):3847–57
- 105. Perez-Gonzalez VH. 2021. Particle trapping in electrically driven insulator-based microfluidics: Dielectrophoresis and induced-charge electrokinetics. *Electrophoresis*. 42(23):2445–64
- 106. Lomeli-Martin A, Ernst OD, Cardenas-Benitez B, Cobos R, Khair AS, Lapizco-Encinas BH. 2023. Characterization of the Nonlinear Electrophoretic Behavior of Colloidal Particles in a Microfluidic Channel. Anal. Chem. 95(16):6740–47
- 107. Antunez-Vela S, Perez-Gonzalez VH, Coll De Peña A, Lentz CJ, Lapizco-Encinas BH. 2020. Simultaneous Determination of Linear and Nonlinear Electrophoretic Mobilities of Cells and Microparticles. *Anal. Chem.* 92(22):14885–91
- 108. Bentor J, Dort H, Chitrao RA, Zhang Y, Xuan X. 2022. Nonlinear electrophoresis of dielectric particles in Newtonian fluids. *Electrophoresis*. 44(11–12):938–46
- Li D. 2004. Electrophoretic motion of particles in microchannels. In *Interface Science and Technology*.
 2(C):542–616
- 110. Cardenas-Benitez B, Jind B, Gallo-Villanueva RC, Martinez-Chapa SO, Lapizco-Encinas BH, Perez-Gonzalez VH. 2020. Direct Current Electrokinetic Particle Trapping in Insulator-Based Microfluidics: Theory and Experiments. *Anal. Chem.* 92(19):12871–79
- Tottori S, Misiunas K, Keyser UF, Bonthuis DJ. 2019. Nonlinear Electrophoresis of Highly Charged Nonpolarizable Particles. *Phys. Rev. Lett.* 123(1):14502
- 112. Rouhi Youssefi M, Diez FJ. 2016. Ultrafast electrokinetics. *Electrophoresis*. 37(5–6):692–98
- Coll De Peña A, Miller A, Lentz CJ, Hill N, Parthasarathy A, et al. 2020. Creation of an electrokinetic characterization library for the detection and identification of biological cells. *Anal. Bioanal. Chem.* 412(16):3935–45
- 114. Xuan X. 2022. Review of nonlinear electrokinetic flows in insulator-based dielectrophoresis: From induced charge to Joule heating effects. 43(1–2):167–189
- 115. Dukhin AS, Dukhin SS. 2005. Aperiodic capillary electrophoresis method using an alternating current electric field for separation of macromolecules. *Electrophoresis*. 26(11):2149–53
- 116. Mishchuk NA, Barinova NO. 2011. Theoretical and experimental study of nonlinear electrophoresis. Colloid J.

- 73(1):88-96
- 117. Lapizco-Encinas BH. 2019. On the recent developments of insulator-based dielectrophoresis: A review. *Electrophoresis*. 40(3):358–75
- 118. Vaghef-Koodehi A, Dillis C, Lapizco-Encinas BH. 2022. High-Resolution Charge-Based Electrokinetic Separation of Almost Identical Microparticles. *Anal. Chem.* 94(17):6451–56
- 119. Hill N, Lapizco-Encinas BH. 2019. On the use of correction factors for the mathematical modeling of insulator based dielectrophoretic devices. *Electrophoresis*. 40(18–19):2541–52
- 120. Sonker M, Kim D, Egatz-Gomez A, Ros A. 2019. Separation Phenomena in Tailored Micro- and Nanofluidic Environments. *Annu. Rev. Anal. Chem.* 12(1):475–500
- 121. Lalonde A, Romero-Creel MF, Lapizco-Encinas BH. 2015. Assessment of cell viability after manipulation with insulator-based dielectrophoresis. *Electrophoresis*. 36(13):1479–84
- 122. Gallo-Villanueva RC, Jesús-Pérez NM, Martínez-López JI, Pacheco A, Lapizco-Encinas BH. 2011. Assessment of microalgae viability employing insulator-based dielectrophoresis. *Microfluid. Nanofluidics*. 10(6):1305–15
- 123. Crowther C V., Hilton SH, Kemp LK, Hayes MA. 2019. Isolation and identification of *Listeria monocytogenes* utilizing DC insulator-based dielectrophoresis. *Anal. Chim. Acta*. 1068:41–51
- 124. Braff WA, Pignier A, Buie CR. 2012. High sensitivity three-dimensional insulator-based dielectrophoresis. *Lab Chip.* 12(7):1327–31
- 125. Zhu J, Canter RC, Keten G, Vedantam P, Tzeng T-RRJ, Xuan X. 2011. Continuous-flow particle and cell separations in a serpentine microchannel via curvature-induced dielectrophoresis. *Microfluid. Nanofluidics*. 11(6):743–52
- Mohammadi M, Madadi H, Casals-Terré J, Sellarès J. 2015. Hydrodynamic and direct-current insulator-based dielectrophoresis (H-DC-iDEP) microfluidic blood plasma separation. *Anal. Bioanal. Chem.* 407(16):4733

 –44
- 127. Liu Y, Jiang A, Kim E, Ro C, Adams T, et al. 2019. Identification of neural stem and progenitor cell subpopulations using DC insulator-based dielectrophoresis. *Analyst.* 144(13):4066–72
- 128. Srivastava SK, Artemiou A, Minerick AR. 2011. Direct current insulator-based dielectrophoretic characterization of erythrocytes: ABO-Rh human blood typing. *Electrophoresis*. 32(18):2530–40
- 129. Braff WA, Willner D, Hugenholtz P, Rabaey K, Buie CR. 2013. Dielectrophoresis-Based Discrimination of Bacteria at the Strain Level Based on Their Surface Properties. *PLoS One*. 8(10):e76751
- 130. Hilton SH, Crowther C V., McLaren A, Smithers JP, Hayes MA. 2020. Biophysical differentiation of susceptibility and chemical differences in: Staphylococcus aureus. *Analyst*. 145(8):2904–14
- Liu Y, Hayes MA. 2020. Differential Biophysical Behaviors of Closely Related Strains of Salmonella. Front. Microbiol. 11:302
- 132. Hilton SH, Hayes MA. 2019. A mathematical model of dielectrophoretic data to connect measurements with cell properties. *Anal. Bioanal. Chem.* 411:2223–37

Figures

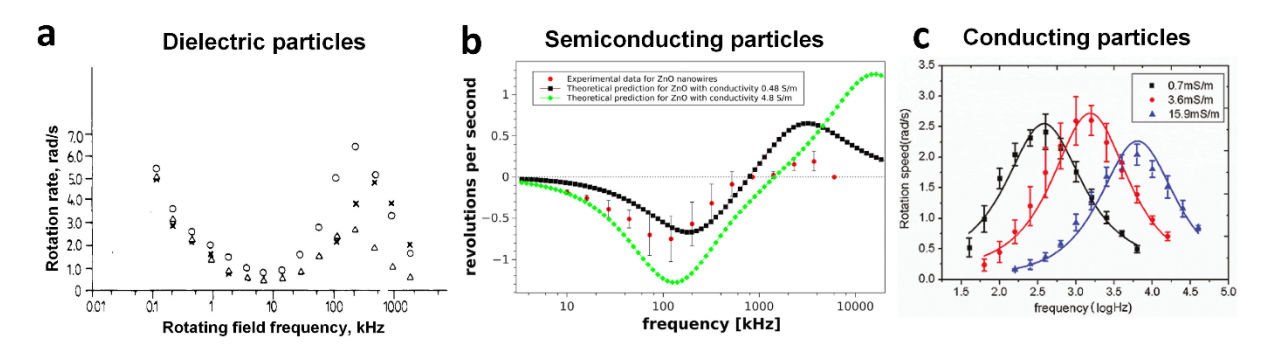


Figure 1

Electrorotation spectra of dielectric, semiconducting and conducting particles. (a) Dielectric particles (polystyrene carboxylated microparticles) depicting two rotation peaks (first peak is just partial) in the cofield direction. The spectra of three distinct particles are shown in the plot: "O" corresponds to 5.29-µm particles in 7 µS/cm medium, "X" corresponds to 5.29-µm particles in 15 µS/cm medium, adapted with permission from Reference (35). Copyright 1987, American Chemical Society. (b) Semiconducting particles (ZnO nanowires) depicting a peak in the counterfield direction at low frequency and a peak in the cofield direction at higher frequency. The red circles are experimental data and predicted data are black and green squares at two distinct media conductivities. Reprinted with permission from Reference (40). Copyright 2017, American Chemical Society. (c) Conducting particles (10-µm gold-coated polystyrene microparticles) in three distinct suspending media conductivity depicting a single rotation speed peak in the counterfield direction (although the velocity is plotted as "positive" – the rotation is counterfield). Reprinted with permission from Reference (43). Copyright 2011, American Chemical Society.

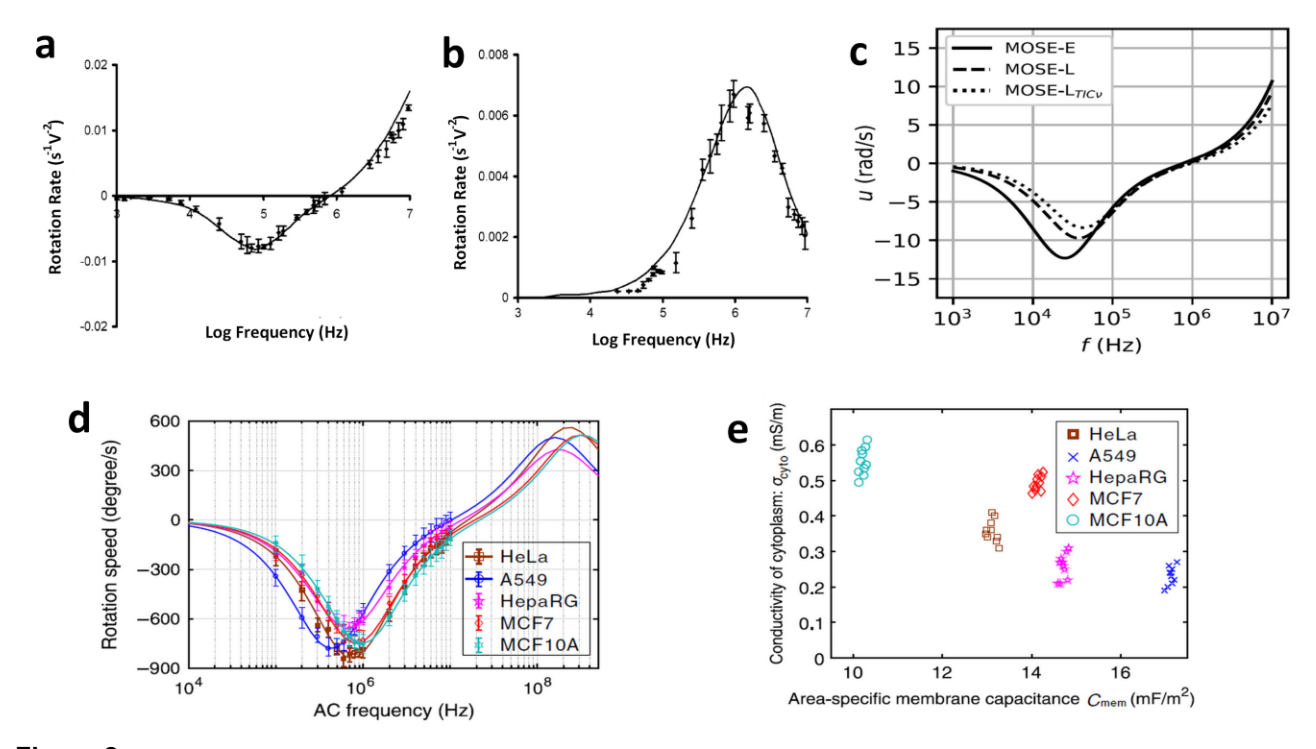


Figure 2

Electrorotation response of cells. (a) Electrorotation spectra of live and (b) non-viable yeast cells. As observed, the behavior changes from counterfield rotations for live cells to cofield rotation for non-viable cells. Adapted with permission from Reference (38). Copyright 2007, Elsevier. (c) Electrorotation spectra of three distinct stages of cancer malignancy of MOSE cells. Adapted from (54), Copyright 2019, Trainito et al. Open access article published under a Creative Commons Attribution License CC BY4.0 DEED. (d) Electrorotation spectra and (e) cytoplasm conductivity as a function of areaspecific membrane capacitance of five types of cancer cells. Adapted from Reference (46). Copyright 2020, Huang et al. Open access article published under a Creative Commons Attribution International License CC BY 4.0 DEED.

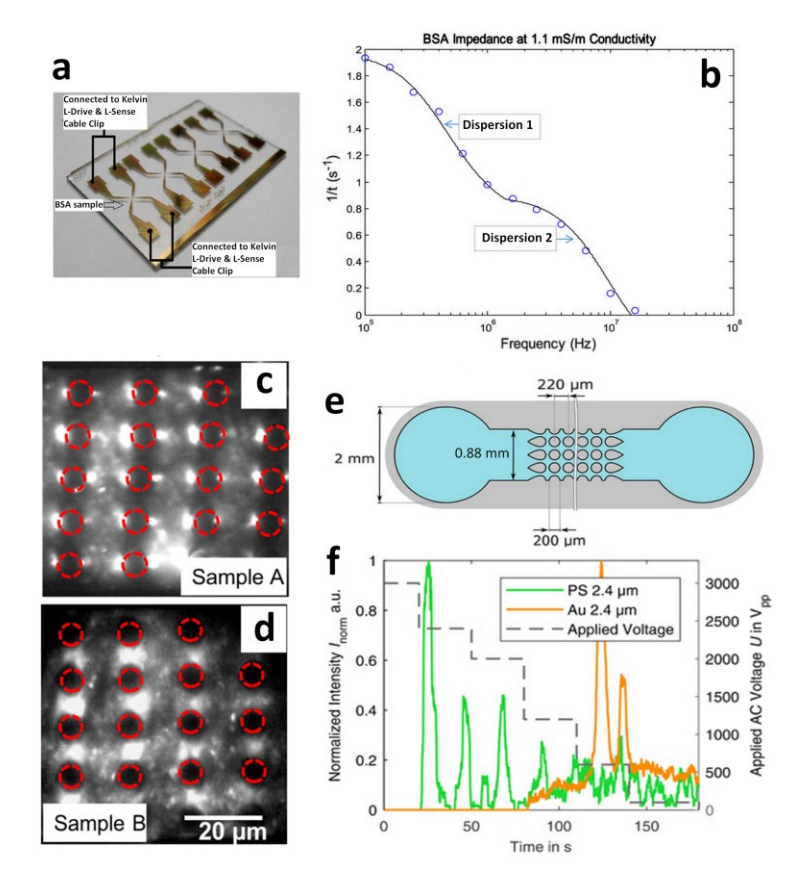


Figure 3

Dielectrophoresis of particles. (a) Microdevice employed for label-free impedance assessment of BSA protein colloidal particles, impedance measurements were performed as protein particles collected between the microelectrodes. (b) Plot of 1/t as a function of frequency showing the two dispersions of the colloidal BSA protein particles in a medium with a conductivity of 1.1 mS/m. Adapted from Reference (71), Copyright 2020, Huang et al. Open access article published under a Creative Commons Attribution license CC BY 4.0 DEED. (c) Negative dielectrophoresis response and (d) positive dielectrophoresis response of DNA-wrapped CNTs under a potential of 1000 V at 700 Hz in an iDEP microchannel. Adapted from Reference (77), Copyright 2017, American Chemical Society, open access article published under an ACS AuthorChoice License. (e) Top view of the iDEP microchannel used for the material-based separation of microparticles. (f) Dielectropherogram of the separation of two types of 2.4 µm (polystyrene and gold-coated polystyrene) microparticles obtained with an AC potential at 10 kHz and DC potential of 100 V. Adapted with permission from Reference (84). Copyright 2019, AIP Publishing.

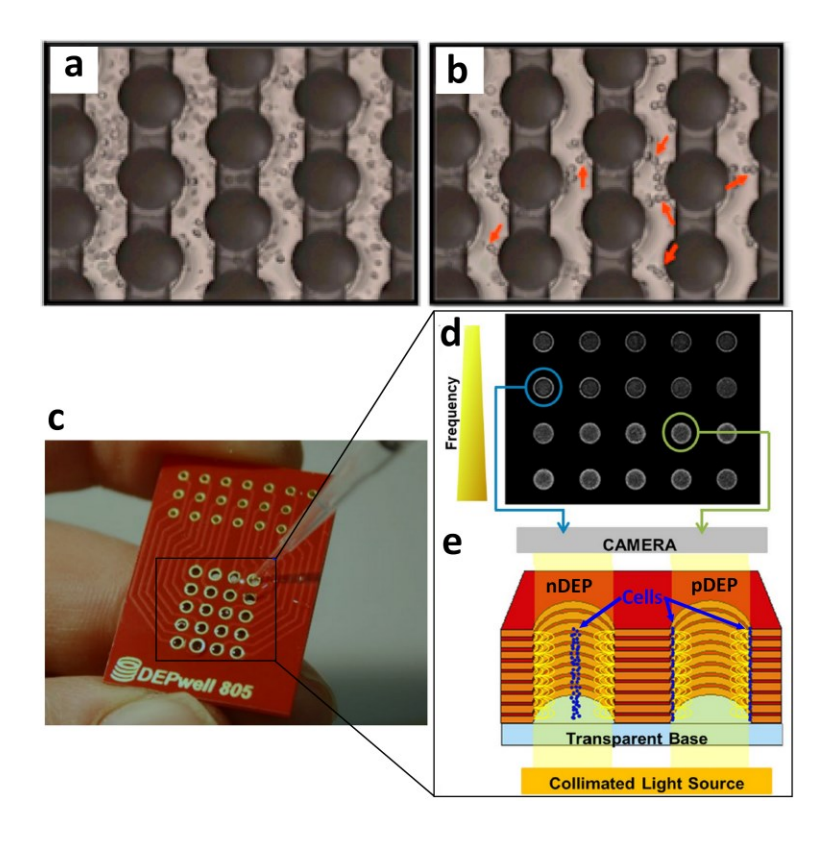


Figure 4

Dielectrophoresis of cells. (a) Non-trapped live and dead monocytes before voltage application and (b) trapped live monocytes after voltage application in the 3D carbon electrode system used by Yildizhan et al. (92). The applied voltage was 20 Vpp at 300 kHz under a flow rate of 1 µL/min. The cylindrical 3D carbon electrodes are on planar SU-8 leads. Image (a) shows both live and dead monocytes, while image (b) shows the trapped live monocytes after dead monocytes were removed. Red arrows show live monocytes in pearl-chain formations. Adapted from Reference (92), Copyright 2017, Yildizhan et al. Open access article published under a Creative Commons Attribution license CC BY 4.0 DEED. (c) 3D dielectrophoresis well chip employed by Hoettges et al. (d) Zoomed-in view of the wells while performing a frequency dependent analysis. (e) Representation of negative dielectrophoresis and positive dielectrophoresis cell behavior as a function of the frequency of the applied potential. Adapted from Reference (98), Copyright 2019, Hoettges et al. Open access article published under a Creative Commons License CC BY 4.0 DEED.

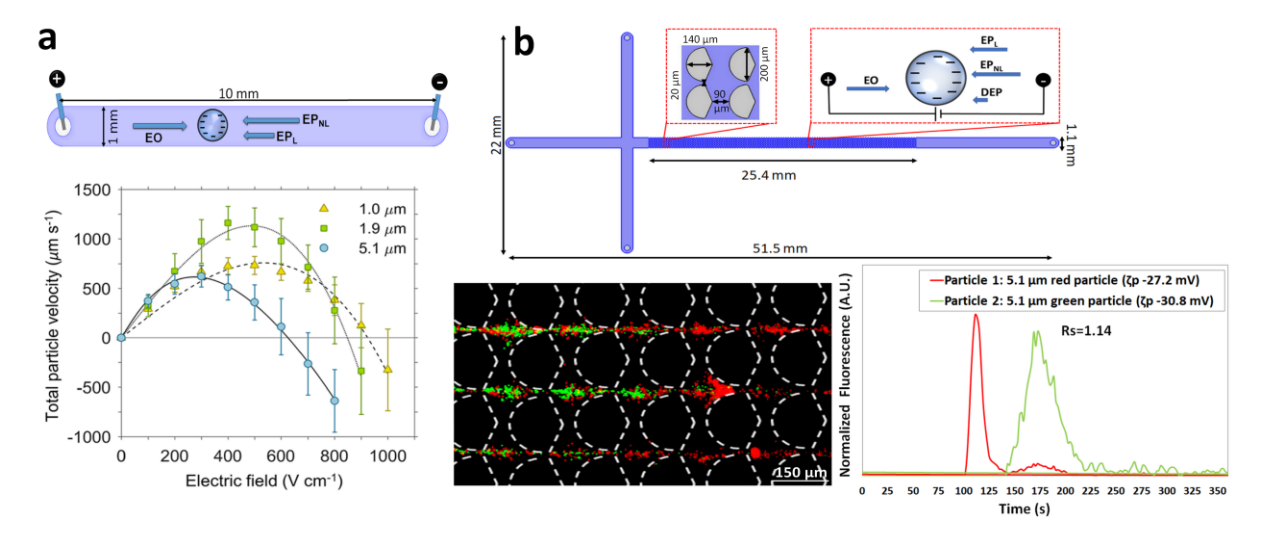


Figure 5

Nonlinear electrophoresis of particles. (a) Microchannel with representation of the forces acting on a negative particle and plot of particle velocity as a function of electric field of three distinct types of microparticles. The velocity plot was adapted from Reference (110), Copyright 2020, American Chemical Society, open access article under the Creative Commons Attribution (CC-BY- NC-ND) 4.0 license. (b) Microchannel with four reservoirs and an array of insulating posts including a representation of the four forces acting on a negative particle, where the terms EO, EP_L, EP_{NL} and DEP refer to electroosmosis, linear electrophoresis, nonlinear electrophoresis and dielectrophoresis, respectively. Image depicting the two types of microparticles, red and green, as they migrate across the post array where red particles are ahead, and electropherogram of the microparticle separation. Separation was carried out by applying a potential of 500 V across the main channel. Adapted with permission from Reference (118), Copyright 2022, American Chemical Society.

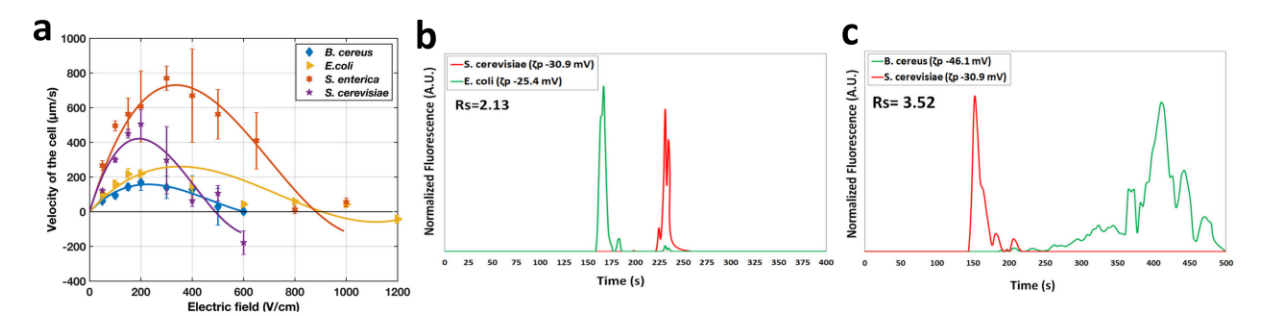


Figure 6

Nonlinear electrophoresis of cells. (a) Plot of cell velocity as a function of electric field of four distinct types of cells. Adapted from Reference (107), Copyright 2020, American Chemical Society (b) Electropherogram of the separation of *E. coli* and *S. cerevisiae* cells carried out by applying a potential of 1000 V across the main channel. (c) Electropherogram of the separation of *B. cereus* and *S. cerevisiae* cells carried out by applying a potential of 500 V across the main channel. Adapted with permission from Reference (8) Copyright 2023, American Chemical Society.